Thermodynamics of a Minimal Algorithmic Cooling Refrigerator

Rodolfo R. Soldati,[1] Durga B. R. Dasari,[2] Jörg Wrachtrup,[2,3] and Eric Lutz[1]

[1]*Institute for Theoretical Physics I, University of Stuttgart, D-70550 Stuttgart, Germany*
[2]*3rd Institute of Physics, IQST, and Research Centre SCoPE, University of Stuttgart, D-70550 Stuttgart, Germany*
[3]*Max Planck Institute for Solid State Research, D-70569 Stuttgart, Germany*

We investigate, theoretically and experimentally, the thermodynamic performance of a minimal three-qubit heat-bath algorithmic cooling refrigerator. We analytically compute the coefficient of performance, the cooling power, and the polarization of the target qubit for an arbitrary number of cycles, taking realistic experimental imperfections into account. We determine their fundamental upper bounds in the ideal reversible limit and show that these values may be experimentally approached using a system of three qubits in a nitrogen-vacancy center in diamond.

Cooling has been an important application of thermodynamics since its foundation. Refrigeration generically occurs when heat is extracted from a system, leading to a decrease of its entropy and a reduction of its temperature below that of the environment [1]. Efficient cooling methods are essential for the study of low-temperature quantum phenomena, from the physics of atoms and molecules [2,3] to novel states of matter [4,5] and the development of quantum technologies [6,7]. In the latter context, the challenge to initialize qubits in pure states with high fidelity has led to the introduction of powerful algorithmic cooling techniques, in which standard quantum logic gates are employed to transfer heat out of a number of spins in order to increase their polarization, both in closed [8] and open [9] systems (see Ref. [10] for a review).

Heat-bath algorithmic cooling is a method that allows us to cool (slow-relaxing) target spins with the help of (fast-relaxing) reset spins that pump entropy out of the target spins into a bath, which acts as an entropy sink [9–20]. An algorithmic cooling cycle consists of a succession of (i) compression steps that cool the target spins and heat up the reset spins, and of (ii) refresh steps during which the reset spins quickly relax back to the bath temperature (Fig. 1). Cyclic algorithmic cooling operation has recently been demonstrated experimentally for a minimal system of three qubits, using nuclear magnetic resonance [21–24] and nitrogen-vacancy centers in diamond [25].

Motivated by these experiments, we here introduce a realistic model of a heat-bath algorithmic cooling refrigerator composed of one target qubit and of two reset qubits [21–25] and investigate its thermodynamic performance. We determine its fundamental limits and compare them to those of standard quantum refrigerators [26–30]. Conventional refrigerators cyclically pump heat from a cold to a hot macroscopic system (both considered as heat baths) by consuming work [1]. Two central figures of merit of

such refrigerators are the coefficient of performance (COP), defined as the ratio of heat extracted and work supplied, and the cooling power that characterizes the rate of heat removal. The maximum value of the COP is given, in the reversible limit, by the ideal Carnot expression, $\zeta_C = T_c/(T_h - T_c)$, where T_c and T_h are the respective temperatures of the cold and hot baths [1]. Algorithmic cooling refrigerators share similarities with conventional quantum refrigerators: they cyclically transfer heat from the cold spins to the hot bath by consuming work done by gate operations. Such analogy makes a comparison between the two refrigerators possible. However, their underlying cooling mechanisms are intrinsically different and the finite size of the target qubit results in a cycle that is not closed in the thermodynamic sense, since its state is not the same at the beginning and at the end of one cycle.

The performance of thermal machines coupled to finite baths with finite heat capacities may be conveniently analyzed with cycle-dependent quantities [32–37]. In the
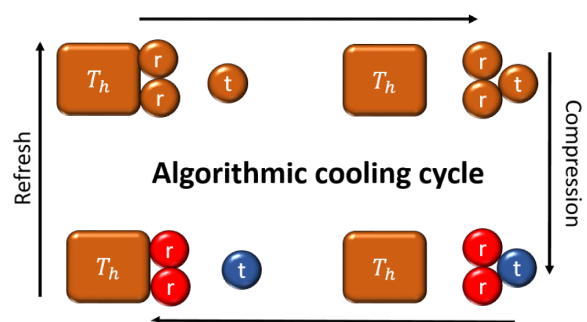

FIG. 1. Schematic illustration of the minimal three-qubit algorithmic cooling cycle: in a first (compression) step, heat is extracted from the target qubit (t), cooling it down while heating up the two reset qubits (r). In a second (refresh) step, the reset qubits are rethermalized to the bath temperature T_h.

following, we compute COP, cooling power, and polarization of the target qubit per cycle for an arbitrary number of cycle iterations. We employ Liouville space techniques [38] to exactly solve the full nonstationary dynamics of the system. While heat-bath algorithmic cooling has been mostly studied in the unitary limit and under steady-state conditions [9–20], we explicitly account for experimentally relevant external damping of the target qubit and for nonideal implementation of logic gates [21–25], for arbitrary cycle numbers including the transient regime. We obtain explicit expressions for the fundamental upper bounds for COP and cooling power in the ideal reversible limit and compare the former to the ideal Carnot COP of a quantum refrigerator [26–29]. Finally, we experimentally determine the performance of the minimal algorithmic cooling refrigerator using three qubits in a nitrogen-vacancy (NV) center in diamond [25] and obtain values of COP and cooling power that are close to their fundamental bounds.

Quantum algorithmic cooling refrigerator.—We consider a minimal three-qubit heat-bath algorithmic cooling refrigerator with Hamiltonian $H = \sum_i \omega_i \sigma_i^z$, where ω_i is the frequency and σ_i^z the usual Pauli operator of each spin. Qubit 1 is the target spin while qubits 2 and 3 are the two reset spins. The machine starts in a separable state of the three qubits, $\rho(0) = \otimes_i \rho_i(0)$, with respective density matrices $\rho_i(0) = \text{diag}[1 - \epsilon_i(0), 1 + \epsilon_i(0)]/2$ and polarizations $\epsilon_i(0)$. We denote by $\tilde{\rho}_i(n)$ the various states after n iterations of the compression stage and by $\rho_i(n)$ those after both compression and refresh steps. We next identify the heat $Q(n)$ extracted during round n with the average energy change of the target qubit, $Q(n) = tr\{\omega_1 \sigma_1^z[\rho_1(n+1) - \rho_1(n)]\}$. We further associate the work performed by the logic gates on the system with the corresponding mean energy variation, $W(n) = \sum_i tr\{\omega_i \sigma_i^z[\tilde{\rho}_i(n+1) - \rho_i(n)]\}$ [14]. The COP per cycle, $\zeta(n)$, is then defined as the ratio of pumped heat and applied work, while the cooling power per cycle, $J(n)$, is given (in units of the cycle time) as the discrete derivative (or forward difference) of the heat:

$$\zeta(n) = -\frac{Q(n)}{W(n)} \quad \text{and} \quad J(n) = Q(n+1) - Q(n). \quad (1)$$

These are the principal quantities of our investigation.

We shall examine the thermodynamic properties of heat-bath algorithmic cooling in the general case where compression is implemented with imperfect gates and the (slow-relaxing) target spin is subjected to irreversible energy dissipation [39]. We will discard irreversible losses of the reset spins because of their much faster relaxation. For each round n of the cooling protocol, we accordingly describe the evolution of the system with the help of three quantum channels [6]. We first account for energy dissipation of the target qubit via an amplitude damping channel $\mathcal{D}$ with decay rate γ [6],

$$\mathcal{D}[\bullet] = \sum_{j=1,2} \Gamma_j \bullet \Gamma_j^\dagger, \quad (2)$$

with the two Kraus damping operators,

$$\Gamma_1 = \begin{pmatrix} 1 & 0 \\ 0 & \sqrt{1-\gamma} \end{pmatrix} \quad \text{and} \quad \Gamma_2 = \begin{pmatrix} 0 & \sqrt{\gamma} \\ 0 & 0 \end{pmatrix}. \quad (3)$$

We further characterize the imperfect compression stage with the channel $\tilde{\rho}(n) = \mathcal{C}[\rho(n-1)]$, such that,

$$\mathcal{C}[\bullet] = \sum_{k=1,2} K_k \bullet K_k^\dagger, \quad (4)$$

where we have introduced the two quantum operators,

$$K_1 = \frac{I}{\sqrt{2}} - \frac{1}{\sqrt{2}}(|011\rangle\langle 011| + |100\rangle\langle 100|)$$
$$- i(\sin\theta|011\rangle\langle 100| + \text{H.c.}), \quad (5)$$

$$K_2 = \frac{I}{\sqrt{2}} + \left(\cos\theta - \frac{1}{\sqrt{2}}\right)|011\rangle\langle 011|$$
$$- \left(\cos\theta - \frac{1}{\sqrt{2}}\right)|100\rangle\langle 100|. \quad (6)$$

Here $|0\rangle$ and $|1\rangle$ are the eigenstates of the spin operators σ_i^z and I denotes the unit operator. The angle θ quantifies the imperfection of the compression step. When $\theta = \pi/2$, we recover ideal compression which swaps the diagonal elements of the density matrix, $U = \exp(-i\pi V/2)$ with $V = |100\rangle\langle 011| + |011\rangle\langle 100|$ [9–20]. The compression operation is commonly implemented experimentally with Toffoli or CNOT gates with imperfect fidelity, which leads θ to deviate from the ideal value $\pi/2$ [21–25]. Finally, we describe the refresh step through [9–20]

$$\rho(n) = \mathcal{R}[\tilde{\rho}(n)] = tr_{23}\{\tilde{\rho}(n)\} \otimes \rho_2(0) \otimes \rho_3(0). \quad (7)$$

The composition of the above three channels yields the combined quantum operation $\mathcal{E}[\bullet]$ which corresponds to one round of the refrigeration algorithm.

Analytical results.—We analytically solve the dynamics generated by the quantum channel $\mathcal{E}[\bullet]$ for an arbitrary number n of algorithmic cooling cycles, using vectorization techniques in Liouville space [38]. In this approach, a density matrix σ is mapped onto a vector $\text{vec}(\sigma)$ (often called supervector) in a higher-dimensional Hilbert space, $\sigma = \sum_{r,s} \sigma_{rs}|r\rangle\langle r| \mapsto \text{vec}(\sigma) = \sum_{r,s} \sigma_{rs}|r\rangle|s\rangle$, where the index r is varied first. The quantum channel, with operator-sum representation $\mathcal{E}[\sigma] = \sum_\mu E_\mu \sigma E_\mu^\dagger$, may then be expressed as $\mathcal{E}(\sigma) = \text{unvec}(\Phi_\mathcal{E}\text{vec}(\sigma))$ with the superoperator $\Phi_\mathcal{E} = \sum_\mu E_\mu \otimes (E_\mu^\dagger)^\intercal$. The advantage of the Liouville space representation is that n iterations of the cooling cycle
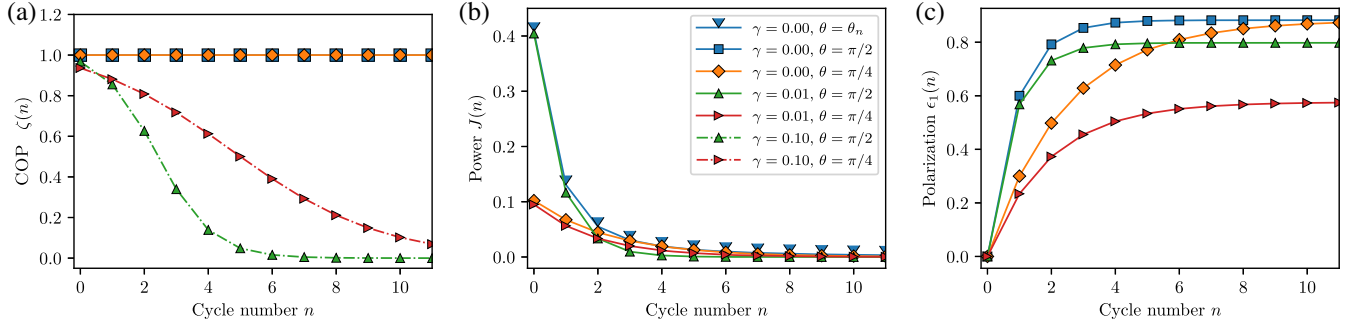
FIG. 2. Thermodynamic performance of the algorithmic cooling refrigerator per cycle. (a) Coefficient of performance $\zeta(n)$, Eq. (8); (b) cooling power $J(n)$, Eq. (8); and (c) polarization of the target qubit $\epsilon_1(n)$, Eq. (9); for various values of the damping rate γ and of the mixing angle θ. These two parameters have radically different effects: whereas the decay constant affects the asymptotic value of the polarization, the mixing angle changes the convergence rate to that value. In addition, the behavior of the cooling power mostly depends on the mixing angle, while the COP depends on both variables. The fundamental upper bounds in the reversible limit ($\gamma = 0$) are shown by the blue squares. Parameters are $\epsilon_1(0) = 0$, $\epsilon_2(0) = \epsilon_3(0) = \epsilon = 0.6$.

may be simply evaluated by computing $\Phi_{\mathcal{E}}^n$, which is not possible in the original Hilbert space (see Supplemental Material [40]). Using this formalism, we obtain explicit expressions for the polarization of the target qubit, as well as for heat and work, from which we deduce COP and cooling

power (1) for each cycle, for arbitrary initial polarizations of the three qubits [40].

For simplicity, we here indicate the formulas for COP and cooling power for the experimentally relevant case of vanishing initial polarization of the target qubit [21–25]:

$$\zeta(n) = \frac{-[2\gamma(1 + \cos^2\theta) - 2\epsilon(2 + \gamma\epsilon)\sin^2\theta][(\gamma - 1)f(\theta) + 4]e^{-ng(\theta,\gamma)}}{\{(\gamma - 1)[f(\theta) + 4(\epsilon^2 + 1)\sin^2\theta] + 4\}\{\gamma f(\theta) + 2\epsilon[\cos(2\theta) - 1]\}e^{-ng(\theta,\gamma)} + 16(1 + \epsilon)^2\gamma\sin^2\theta} \xrightarrow{\gamma=0} \zeta_{\max}(n) = 1$$

$$J(n) = \frac{1}{16}[(\gamma - 1)f(\theta) + 4][4\epsilon\sin^2\theta - \gamma f(\theta)]e^{-ng(\theta,\gamma)} \xrightarrow[\theta=\theta_n]{\gamma=0} J_{\max}(n) = \frac{\epsilon}{2}(1 + \epsilon^2)e^{-ng(\theta_n,0)}, \tag{8}$$

where we have defined the two functions $f(\theta) = 3 + (1 + \epsilon^2)\cos(2\theta) - \epsilon^2$ and $g(\theta, \gamma) = \ln\{4/[(1 - \gamma)f(\theta)]\}$, and introduced the angle $\theta_n = \pi/2$ for $n < 2$, $\epsilon < \sqrt{1/3}$ and $\theta_n = \arccos\{(2\epsilon^2 + n\epsilon^2 + n - 6)/[(2 + n)(1 + \epsilon^2)]\}/2$ otherwise. We have here set $\epsilon_1(0) = 0$, $\epsilon_2(0) = \epsilon_3(0) = \epsilon$ (results for general polarizations are given in Ref. [40]).

Figures 2(a) and 2(b) represent $\zeta(n)$ and $J(n)$ as a function of the cycle number n for various values of the decay rate γ and of the mixing angle θ. We first note that both quantities reach their fundamental maximum values in the undamped limit $\gamma = 0$. In this unitary, reversible regime, the COP $\zeta(n)$ is equal to one, implying that the extracted heat is precisely given by the work supplied by the gate operations, $-Q(n) = W(n)$ (when $\gamma = 0$). The value of $\zeta_{\max}(n)$ is moreover independent of the cycle number n and of the angle θ. This interesting point reveals that gate imperfections do not affect the maximum efficiency of the algorithmic cooling refrigerator, but only reduce the power $J_{\max}(n)$. We further observe that the cooling power generically decays exponentially to zero with increasing cycle iterations, as the asymptotic temperature is reached and no more heat can be extracted from the target qubit—a behavior also exhibited by $\zeta(n)$ in the

presence of irreversible losses. Figure 2(b) additionally shows that $J(n)$ is mostly affected by the angle θ and not so much by the decay rate γ in the experimentally relevant range $\gamma < 0.01$. In particular, the optimal angle θ_n in $J_{\max}(n)$ depends on n for $n \geq 2$ [48].

Two important features of the algorithmic cooling protocol are the asymptotic polarization of the target qubit and the number of iterations needed to reach it [9–20]. Using the Liouville space solution, we find the exact expression [again for $\epsilon_1(0) = 0$, $\epsilon_2(0) = \epsilon_3(0) = \epsilon$] [40],

$$\epsilon_1(n) = \frac{\gamma f(\theta) + 2\epsilon[\cos(2\theta) - 1]}{(\gamma - 1)f(\theta) + 4}[e^{-ng(\theta,\gamma)} - 1]$$

$$\xrightarrow[\theta=\pi/2]{\gamma=0} \epsilon_{1\max}(n) = \frac{2\epsilon}{1 + \epsilon^2}[1 - e^{-ng(\pi/2,0)}]. \tag{9}$$

The stationary value $\epsilon_1(\infty)$ is thus approached exponentially with a rate constant given by $1/g(\theta, \gamma)$. Figure 2(c) displays a radically different effect of energy dissipation and of gate imperfection on the nonideal polarization of the target qubit. While the decay constant γ affects the asymptotic value of the polarization $\epsilon_1(\infty)$, the mixing angle θ modifies the convergence rate to that value for

$\gamma = 0$. As a consequence, imperfect gate operation does not prevent achieving maximum polarization in the reversible limit, it only increases the number of required iterations. This property holds for all convex combinations of the ideal compression and the identity [40].

Let us next compare the thermodynamic performance of the algorithmic cooling refrigerator to that of a conventional quantum refrigerator [26–29], whose COP is upper bounded by the Carnot formula, $\zeta_C = T_c/(T_h - T_c)$. We accordingly evaluate, for each cycle n, the temperature of the target qubit via $T_c(n) = 1/\ln[(1 + \epsilon_1(n))/(1 - \epsilon_1(n))]$, determined via the ratio of the (Boltzmann distributed) populations of excited and ground states (a similar formula holds for the initial hot temperature of the reset spins). The corresponding Carnot COP per cycle, $\zeta_C(n) = T_c(n)/[T_h - T_c(n)]$ for the algorithmic cooling refrigerator is shown, together with the COP $\zeta(n)$, Eq. (8), in Fig. 3. While $\zeta(n)$ is smaller than $\zeta_C(n)$ at the beginning of the refrigeration cycle, the Carnot bound is quickly approached after only a few iterations in the ideal limit ($\gamma = 0, \theta = \pi/2$). The Carnot limit is in general not attained in the presence of damping ($\gamma \neq 0$).

Experimental results.—Finally, we experimentally validate our new theoretical framework, and analyze the performance of an algorithmic cooling refrigerator made of three nuclear spins that are hyperfine coupled to the central electron spin of a NV center in diamond [25]. NV center systems offer excellent control of their states and exhibit very long spin coherence times [49]. The target spin and the two reset spins are respectively chosen to be the nitrogen ^{14}N and two carbon ^{13}C nuclear spins that are coupled to the central electron spin of the NV center with respective strengths 2.16 MHz, 90 kHz, and 414 kHz (Fig. 4). The central electron spin has a twofold role: it acts as (i) the heat bath and also as (ii) an ancillary spin that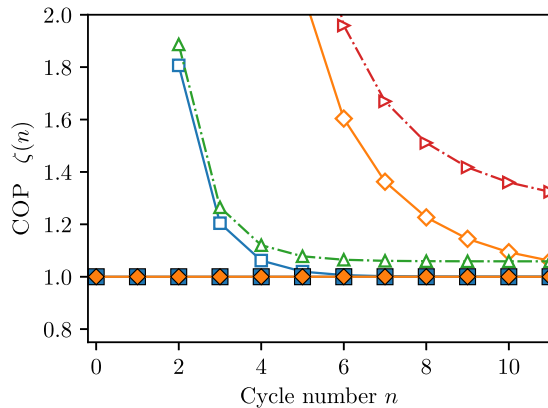 drives the interaction among the spins required to achieve the entropy compression on the target qubit [25]. The optical spin polarization of the central NV spin is transferred to the two ^{13}C spins via a SWAP gate during the refresh steps [40]. Compression is implemented by performing a nonlocal gate among the three nuclear spins that allow for a unitary mixing of populations in the subspace of $[|011\rangle, |100\rangle]$ [40]. As the nuclear spins do not interact with each other, this three qubit Toffoli gate is mediated by the electron spin.

Typical times of each step are $\sim$285 μs for the compression step and $\sim$5 ms for the refresh step. The lifetime of the nuclear spin, T_1, is of the order of seconds (corresponding to a decay rate $\gamma \simeq 10^{-4}$), allowing us to perform multiple rounds of the cooling cycle. Since the refresh step periodically resets the two ^{13}C spins, their damping is not relevant over the duration of the experiment. Another source of noise, not considered in previous experiments [21–24], is due to imperfect compression: the compression algorithm indeed utilizes three-qubit Toffoli gates [25],

FIG. 3. Comparison with the Carnot coefficient of performance. In the reversible regime ($\gamma = 0$), the coefficient of performance $\zeta(n)$ (full symbols) gets close to the corresponding Carnot limit $\zeta_C(n)$ (empty symbols) after a few cycles. The Carnot bound is generally not reached in the presence of losses ($\gamma \neq 0$). Same parameters as in Fig. 2.
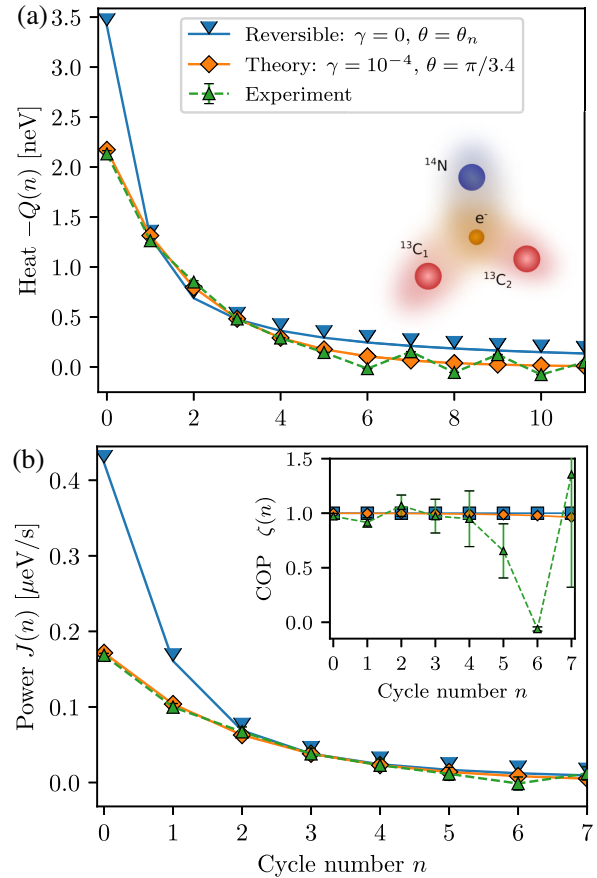
FIG. 4. Experimental performance of the three-qubit algorithmic cooling refrigerator. (a) Experimental data for heat $Q(n)$ (green triangles) show excellent agreement with theory (orange diamond) with $\gamma = 10^{-4}$ and $\theta = \pi/3.4$. (b) Cooling power $J(n)$ and COP $\zeta(n)$ also agree very well with theory [$\zeta(n)$ becomes sensitive to measurement errors for larger n]. Error bars correspond to the standard deviation.

which when transpiled into the electron-nuclear spin gates, involve 5 CNOT gates and 14 single-qubit rotations. Gate imperfections, together with imperfect charge state initialization, lead to mixing between the states $|011\rangle$ and $|100\rangle$, which can be quantified by an effective mixing angle θ. The best fit in our experiment is $\theta \simeq \pi/3.4$, which corresponds to an overall error of $\sim 20\%$ in the compression step. Reset is additionally implemented via an iterative SWAP gate that allows for $\sim 99\%$ fidelity on the achievable hot spin polarization.

The initial polarizations of the two reset spins are $\epsilon_2(0) \sim 0.58$ and $\epsilon_3(0) \sim 0.41$. The imbalance between the polarizations comes from the different coupling strengths of the two spins to the electron spin. We measure the target spin polarization via single-shot readout with a fidelity of $\sim 97\%$, from which we evaluate heat $Q(n)$ and cooling power $J(n)$, as well as work $W(n)$ and COP $\zeta(n)$ for each cycle (see Supplemental Material [40]) [50]. We obtain excellent agreement between theory (with $\gamma = 10^{-4}$ and $\theta = \pi/3.4$) and data [Figs. 4(a) and 4(b)]. We observe especially that the upper bounds $J_{\max}(n)$ and $\zeta_{\max}(n)$, given by Eq. (8), are reached in the experiment. For $n \geq 5$, heat and work are very small. As a result, the COP becomes highly sensitive to measurement errors: it can get negative for $-Q(n)$ below zero (as for $n = 6$) or be larger than one if $W(n)$ is too close to zero (as for $n = 7$).

Conclusions.—We have performed a theoretical and experimental study of the thermodynamic performance of a minimal three-qubit algorithmic cooling refrigerator. We have analytically computed key figures of merit, such as coefficient of performance, cooling power, and polarization of the target qubit, for an arbitrary number of cycles. We have determined their fundamental upper bounds in the ideal reversible limit and shown that the coefficient of performance quickly converges to the Carnot value after a few cycles. We have further highlighted the effects of realistic experimental imperfections, in particular, irreversible energy dissipation of the target qubit and imperfect gate operations, on these quantities. Finally, we have demonstrated that the fundamental limits may be approached in an experimental system made of the three qubits of a NV center in diamond.

[1] H. B. Callen, *Thermodynamics and an Introduction to Thermostatistics* (Wiley, New York, 1985).

[2] H. J. Metcalf and P. van der Straten, *Laser Cooling and Trapping* (Springer, Berlin, 1999).

[3] V. S. Letokhov, *Laser Control of Atoms and Molecules* (Oxford University Press, Oxford, 2007).

[4] P. V. E. McClintock, D. J. Meredit, and J. K. Wigmore, *Low-Temperature Physics* (Springer, Berlin, 1992).

[5] C. Ens and S. Hunklinger, *Low-Temperature Physics* (Springer, Berlin, 2005).

[6] M. A. Nielsen and I. L. Chuang, *Quantum Computation and Quantum Information* (Cambridge University Press, Cambridge, England, 2000).

[7] E. Desurvire, *Classical and Quantum Information Theory* (Cambridge University Press, Cambridge, England, 2009).

[8] L. J. Schulman and U. V. Vazirani, Molecular scale heat engines and scalable quantum computation, in *Proceedings of the 31st ACM Symposium on Theory of Computing* (ACM Press, New York, 1999), p. 322.

[9] P. O. Boykin, T. Mor, V. Roychowdhury, F. Vatan, and R. Vrijen, Algorithmic cooling and scalable NMR quantum computers., Proc. Natl. Acad. Sci. U.S.A. **99**, 3388 (2002).

[10] D. K. Park, N. A. Rodríguez-Briones, G. Feng, R. R. Darabad, J. Baugh, and R. Laflamme, Heat bath algorithmic cooling with spins: Review and prospects, in *Electron Spin Resonance (ESR) Based Quantum Computing*, Biological Magnetic Resonance Vol. 31 (Springer, New York, 2016), pp. 227–255.

[11] J. M. Fernandez, S. Lloyd, T. Mor, and V. Roychowdhury, Algorithmic cooling of spins: A practicable method for increasing polarization, Int. J. Quantum. Inform. **02**, 461 (2004).

[12] L. J. Schulman, T. Mor, and Y. Weinstein, Physical Limits of Heat-Bath Algorithmic Cooling, Phys. Rev. Lett. **94**, 120501 (2005).

[13] L. J. Schulman, T. Mor, and Y. Weinstein, Physical limits of heat-bath algorithmic cooling, SIAM J. Comput. **36**, 1729 (2007).

[14] F. Rempp, M. Michel, and G. Mahler, Cyclic cooling algorithm, Phys. Rev. A **76**, 032325 (2007).

[15] P. Kaye, Cooling algorithms based on the 3-bit majority, Quantum Inf. Process. **6**, 295 (2007).

[16] G. Brassard, Y. Elias, T. Mor, and Y. Weinstein, Prospects and limitations of algorithmic cooling, Eur. Phys. J. Plus **129**, 258 (2014).

[17] S. Raeisi and M. Mosca, Asymptotic Bound for Heat-Bath Algorithmic Cooling, Phys. Rev. Lett. **114**, 100404 (2015).

[18] N. A. Rodríguez-Briones and R. Laflamme, Achievable Polarization for Heat-Bath Algorithmic Cooling, Phys. Rev. Lett. **116**, 170501 (2016).

[19] S. Raeisi, M. Kieferov, and M. Mosca, Novel Technique for Robust Optimal Algorithmic Cooling, Phys. Rev. Lett. **122**, 220501 (2019).

[20] S. Raeisi, No-go theorem behind the limit of the heat-bath algorithmic cooling, Phys. Rev. A **103**, 062424 (2021).

[21] J. Baugh, O. Moussa, C. A. Ryan, A. Nayak, and R. Laflamme, Experimental implementation of heat-bath algorithmic cooling using solid-state nuclear magnetic resonance, Nature (London) **438**, 470 (2005).

[22] C. A. Ryan, O. Moussa, J. Baugh, and R. Laflamme, Spin Based Heat Engine: Demonstration of Multiple Rounds of Algorithmic Cooling, Phys. Rev. Lett. **100,** 140501 (2008).

[23] D. K. Park, G. Feng, R. Rahimi, S. Labruyere, T. Shibata, S. Nakazawa, K. Sato, T. Takui, R. Laflamme, and J. Baugh, Hyperfine spin qubits in irradiated malonic acid: Heat-bath algorithmic cooling, Quantum Inf. Process. **14,** 2435 (2015).

[24] Y. Atia, Y. Elias, T. Mor, and Y. Weinstein, Algorithmic cooling in liquid-state nuclear magnetic resonance, Phys. Rev. A **93,** 012325 (2016).

[25] S. Zaiser, C. T. Cheung, S. Yang, D. B. R. Dasari, S. Raeisi, and J. Wrachtrup, Cyclic cooling of quantum systems at the saturation limit, npj Quantum Inf. **7,** 92 (2021).

[26] R. Kosloff and A. Levy, Quantum heat engines and refrigerators: Continuous devices, Annu. Rev. Phys. Chem. **65,** 365 (2014).

[27] Y. Rezek, P. Salamon, K. H. Hoffmann, and R. Kosloff, The quantum refrigerator: The quest for absolute zero, Europhys. Lett. **85,** 30008 (2009).

[28] A. E. Allahverdyan, K. Hovhannisyan, and G. Mahler, Optimal refrigerator, Phys. Rev. E **81,** 051129 (2010).

[29] O. Abah and E. Lutz, Optimal performance of a quantum Otto refrigerator, Europhys. Lett. **113,** 60002 (2016).

[30] An information-theoretic analysis of the performance of heat-bath algorithmic cooling, viewed from the perspective of feedback cooling, has been presented in Ref. [31].

[31] P. Liuzzo-Scorpo, L. A. Correa, R. Schmidt, and G. Adesso, Thermodynamics of quantum feedback cooling, Entropy **18,** 48 (2016).

[32] M. J. Ondrechen, B. Andresen, M. Mozurkewich, and R. S. Berry, Maximum work from a finite reservoir by sequential Carnot cycles, Am. J. Phys. **49,** 681 (1981).

[33] Y. Wang, Optimizing work output for finite-sized heat reservoirs: Beyond linear response, Phys. Rev. E **93,** 012120 (2016).

[34] H. Tajima and M. Hayashi, Finite-size effect on optimal efficiency of heat engines, Phys. Rev. E **96,** 012128 (2017).

[35] A. Pozas-Kerstjens, E. G. Brown, and K. V. Hovhannisyan, A quantum Otto engine with finite heat baths: Energy, correlations, and degradation, New J. Phys. **20,** 043034 (2018).

[36] M. H. Mohammady and A. Romito, Efficiency of a cyclic quantum heat engine with finite-size baths, Phys. Rev. E **100,** 012122 (2019).

[37] Y. H. Ma, Effect of finite-size heat source's heat capacity on the efficiency of heat engine, Entropy **22,** 1002 (2020).

[38] J. A. Gyamfi, Fundamentals of quantum mechanics in Liouville space, Eur. J. Phys. **41,** 063002 (2020).

[39] An abstract error analysis of heat-bath algorithmic cooling has been performed in Ref. [15].

[40] See Supplemental Material at http://link.aps.org/supplemental/10.1103/PhysRevLett.129.030601 for further details on the mathematical formalism used and details on the experimental implementation [41–47].

[41] A. Gilchrist, D. R. Terno, and C. J. Wood, Vectorization of quantum operations and its use, arXiv:0911.2539.

[42] R. A. Horn and C. R. Johnson, *Matrix Analysis* (Cambridge University Press, Cambridge, England, 2012).

[43] I. Bengtsson and K. Zyczkowski, *The Geometry of Quantum States* (Cambridge University Press, Cambridge, England, 2006).

[44] V. Vorobyov, S. Zaiser, N. Abt, J. Meinel, D. Dasari, P. Neumann, and J. Wrachtrup, Quantum Fourier transform for nanoscale quantum sensing, npj Quantum Inf. **7,** 124 (2021).

[45] P. Neumann J. Beck, M. Steiner, F. Rempp, H. Fedder, P. R. Hemmer, J. Wrachtrup, and F. Jelezko, Single-shot readout of a single nuclear spin, Science **329,** 542 (2010).

[46] S. Machnes, U. Sander, S. J. Glaser, P. de Fouquières, A. Gruslys, S. Schirmer, and T. Schulte-Herbrüggen, Comparing, optimizing, and benchmarking quantum-control algorithms in a unifying programming framework, Phys. Rev. A **84,** 022305 (2011).

[47] G. Waldherr, Y. Wang, S. Zaiser, M. Jamali, T. Schulte-Herbrüggen, H. Abe, T. Ohshima, J. Isoya, J. F. Du, P. Neumann, and J. Wrachtrup, Quantum error correction in a solid-state hybrid spin register, Nature (London) **506,** 204 (2014).

[48] The decreasing values of θ_n with the cycle number n reduce the rate of exponential decay $g(\gamma, \theta)$ of the power $J(n)$ at each step toward the steady state.

[49] M. W. Doherty, N. B. Manson, P. Delaney, F. Jelezko, J. Wrachtrup, and L. C. L. Hollenberg, The nitrogen-vacancy colour centre in diamond, Phys. Rep. **528,** 1 (2013).

[50] With the Larmor frequency of the target spin (^{14}N) being ~1.66 MHz and a cycle time including compression and reset steps of about ~5 ms, the heat $Q(n)$ extracted per cycle is on the order of a few neV, and the power $J(n)$ is on the order of a few μeV/s or 10^{-26} W.